EuroSun2026

LAB-SCALE EXPERIMENTAL SETUP FOR CHARACTERIZING THERMOCHEMICAL REACTIONS IN SALT HYDRATE MATERIALS

S.E. Cruz Lopez[1]*, S.G. Van der Vaart[1], A.S. Purandare[1], A. Mahmoudi[1], C.W. Visser[1], M. Shahi[1]

[1]*University of Twente, Department of Thermal and Fluid Engineering, Enschede, The Netherlands*

**Corresponding author: s.e.cruzlopez@utwente.nl*

Summary

Thermochemical heat storage (TCS) using salt hydrates theoretically offers, under ideal conditions, high energy density and near-zero thermal loss for integration of sustainable sources to energy requirements in society. However, translating micro-scale material characterization to practical devices remains challenging due to macro-scale heat and mass transfer resistance, agglomeration, and volumetric expansion. To bridge this gap, this paper presents a lab-scale reactor setup for direct and dynamic characterization of thermochemical reactions. The system couples a vacuum-insulated fixed-bed reactor directly with a precision mass scale for macro-gravimetric tracking, supported by continuous inlet and outlet temperature and relative humidity (RH) monitoring.

The methodology was experimentally validated using anhydrous calcium chloride ($CaCl_2$) under controlled airflow conditions (20 °C and 10% RH). Results demonstrated high repeatability, with real-time gravimetric measurements accurately capturing moisture absorption dynamics. The continuous mass tracking closely matched offline post-experiment verifications within a 1% deviation. The contribution of this work is the integration and validation of continuous macro-gravimetric measurement within an operating fixed-bed salt-hydrate reactor, enabling direct measurement of bulk water uptake simultaneously with transient inlet/outlet temperature and humidity.

Keywords: Thermochemical Heat Storage, Salt Hydrates, Reaction Extent, Lab-Scale Reactor, Calcium Chloride.

Field of application for the findings: Thermal Energy Storage for integration of renewable energy sources or industrial waste heat.

Addressed audience: Researchers in thermochemical heat storage, energy systems engineers, and industrial developers working on reaction systems.

1. Introduction

The transition to sustainable energy requires the effective integration of renewable sources, such as solar and wind power. However, their intermittent nature creates a temporal mismatch between energy generation and industrial or residential demand. As noted by Schermeyer et al. (2018), several European Union (EU) countries already face significant imbalances between energy supply and grid distribution capacities.

Thermochemical Heat Storage (TCS) offers a promising solution to address these seasonal and daily energy mismatches. Compared to other thermal storage methods, TCS stands out due to its high energy density and near-zero thermal losses over long-term storage periods (Tafere (2026)).

Salt hydrates are particularly promising for domestic heat storage applications. As shown in Equation 1, these reversible hydration reactions absorb and release large amounts of heat, making them a great fit for solar energy availability and home heating needs.

$$Salt \cdot \alpha H_2O(s) + (\beta - \alpha)H_2O(g) \underset{\text{dehydration}}{\overset{\text{hydration}}{\rightleftharpoons}} Salt \cdot \beta H_2O(s) + Heat \quad (1)$$

However, translating fundamental TCS research on salt hydrate materials and their reaction kinetics and mass transfer limitations into commercial applications remains challenging. Most studies characterizing salt hydrates rely on milligram-scale techniques, such as Thermogravimetric Analysis (TGA) and Differential Scanning Calorimetry (DSC) (Opel et al. (2011)). These micro-scale tests fail to predict real-world reactor performance because they assume uniform heating and unrestricted gas flow, omitting bulk physical constraints such as intra-bed heat and mass transfer resistance, material agglomeration, deliquescence, and volume expansion. In practical systems, macro-scale phenomena significantly impact performance and must be accounted for.

Because developing full-scale industrial or domestic prototypes is often cost-prohibitive, lab-scale reactors serve as a crucial bridge. They help connect micro-scale material analyses with the complex behavior of upscaled systems. By capturing the macro-scale phenomena omitted in fundamental tests, lab-scale data enables a direct comparison that helps identify technical bottlenecks and practical limitations before full commercialization.

Current literature describes various methods for monitoring reactor performance by measuring the thermal power transferred to or from the heat transfer fluid. As demonstrated by Stengler et al. (2021), Kur et al. (2023), and Uykun et al. (2026), mass balances of the substances involved in the thermochemical reaction and their corresponding reaction velocities according to those punctual concentrations over time can be estimated using reaction stoichiometry. While this approach provides a useful initial approximation of intra-reactor processes, it often relies on assumptions to account for uncontrolled environmental heat losses, which can lead to less accurate representations of the true reaction dynamics.

To improve the accuracy of these studies, this paper develops and experimentally validates a lab-scale fixed-bed reactor incorporating continuous macro-gravimetric measurement. The objective is to determine whether bulk water uptake can be measured reliably during hydration while simultaneously monitoring the inlet and outlet temperature and humidity response. The method is evaluated using repeated hydration experiments with anhydrous $CaCl_2$, and the gravimetrically measured final water uptake is independently verified using an external balance.

2. Experiments

The investigation presented in this paper is supported by experimental data gathered using a setup developed to measure three different quantities, namely temperature and humidity of the working fluid, and mass dynamics in the salt hydrate materials, as detailed in the section below.

2.1 Experimental setup

To accurately investigate the performance of the thermochemical material (TCM) under specific reacting conditions, a reaction chamber was designed and built to provide precise control over flow rate and temperature of the heat transfer fluid, and the water concentration injected into the reaction system, which are the variables governing the process's mass and heat transfer. Figure 1 presents a schematic overview of the experimental system.

The system features a humidifier unit that supplies air at controlled temperature and humidity levels. Humidification is achieved by passing a calculated proportion of dry air through a water bubble column. This saturated air is then mixed with a regulated quantity of dry air to reach the target moisture content. The conditioned air (working fluid) is then directed into the reaction chamber: a vacuum-insulated borosilicate glass reactor equipped with a bottom gas dispersion plate.

The reactor is mounted on a mass scale, featuring a maximum capacity of 6200 g and a resolution of 0.1 g, to continuously monitor mass changes during the experiment. Additionally, temperature and humidity sensors (operating range: -40 to 80 °C with an accuracy of ±0.1 °C, and 0 to 100% RH with an accuracy of ±1.5% RH, respectively) are installed at the reactor inlet and suspended near the reactor outlet (at a safe distance from the solid reactants) to track the entry and exit conditions of the working fluid. A precisely measured amount

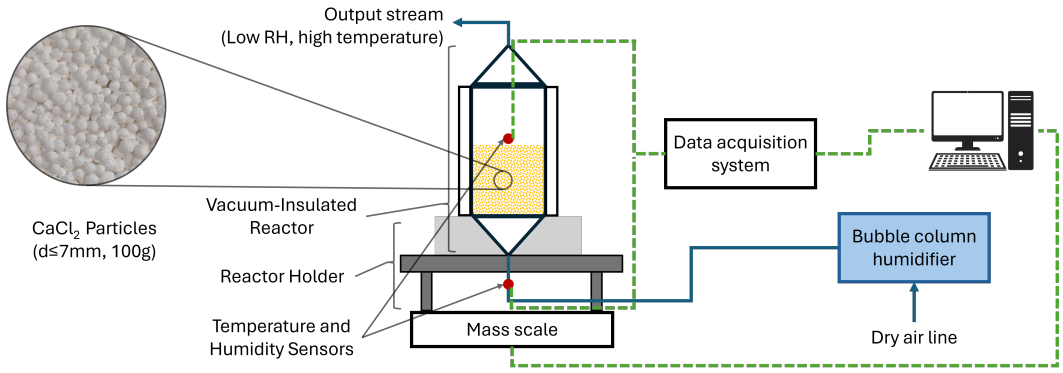

Fig. 1: Schematic of the lab-scale heat storage experimental setup employing a mass scale coupled to the reaction vessel to live-track the water intake in the TCM ($CaCl_2$ Particles) and a Humidifier system which supplies moisturized air in specific temperature and RH conditions. Dotted lines represent the data channels which communicate the sensed information with the corresponding post-processing units.

of solid TCM is loaded directly into the reactor during the experiment run. The sensors and the mass scale interface with a computer system for continuous data logging. During installation, the cables and tubing were clamped to an external frame to prevent direct contact with the mass scale's measuring plate, ensuring the instrumentation did not interfere with gravimetric measurements.

Figure 2 provides a detailed piping and instrumentation diagram (P&ID) of the experimental test system, containing two main subsystems. The control subsystem ensures the required temperature and humidity conditions at the inlet of the test-section. The test-section consists of the reactor and sensor arrangements. The corresponding components are listed in Table 1, and the process stream conditions are described in Table 2.

2.2 Materials

Anhydrous calcium chloride ($CaCl_2$) (Sigma-Aldrich, granular, ≤ 7.0 mm, ≥93.0%) was used as the TCM. Demineralized water was loaded into the humidifier's bubble column to supply moisture to the airflow.

2.3 Macro-gravimetric method preparations

The operation of this experimental setup requires structuring two execution phases, where the first is required to prepare the internal components of the gravimetric sensing system, and the subsequent phase is to properly obtain the data of the chemical process.

First, the mass scale must be conditioned to the operating environment. Because the scale is highly sensitive and the setup's total weight significantly exceeds the expected mass of reacting water vapor, the scale's internal load cell undergoes an initial mechanical deformation (Sulistyanto et al. (2017)). When subjected to loads an order of magnitude higher than the expected reaction mass gains, the load sensor exhibits mechanical relaxation. This drift causes an apparent continuous mass loss that outweighs and masks the smaller mass gain occurring in the fixed bed.

To account for this, the TCM is loaded into the reactor before it is assembled on the scale. For all experiments reported here, 100 grams of solid TCM was portioned and loaded as a fixed bed using a 3D-printed holder. This holder is a Nylon cylinder featuring a removable perforated bottom plate. A rubber O-ring seals the cylinder against the reactor's inner wall, preventing air from bypassing the salt bed. The preparation stage was considered complete once the residual mass drift remained below 0.5 g/h over a period of 3 h. Under the conditions investigated, this criterion was typically reached after approximately 12 h.

The initial deformation of the scale's Wheatstone bridge, as described by Sulistyanto et al. (2017), is visible in Figure 3A. The apparent mass of the system gradually drifts before stabilizing during the preparation phase. Once stabilized, the gravimetric device is ready to accurately measure gradual water uptake. Figure 3B illustrates the steady-state baseline achieved across three separate batches. This demonstrates that the system reaches stable conditions prior to hydration, ensuring that any recorded mass changes are driven solely by the

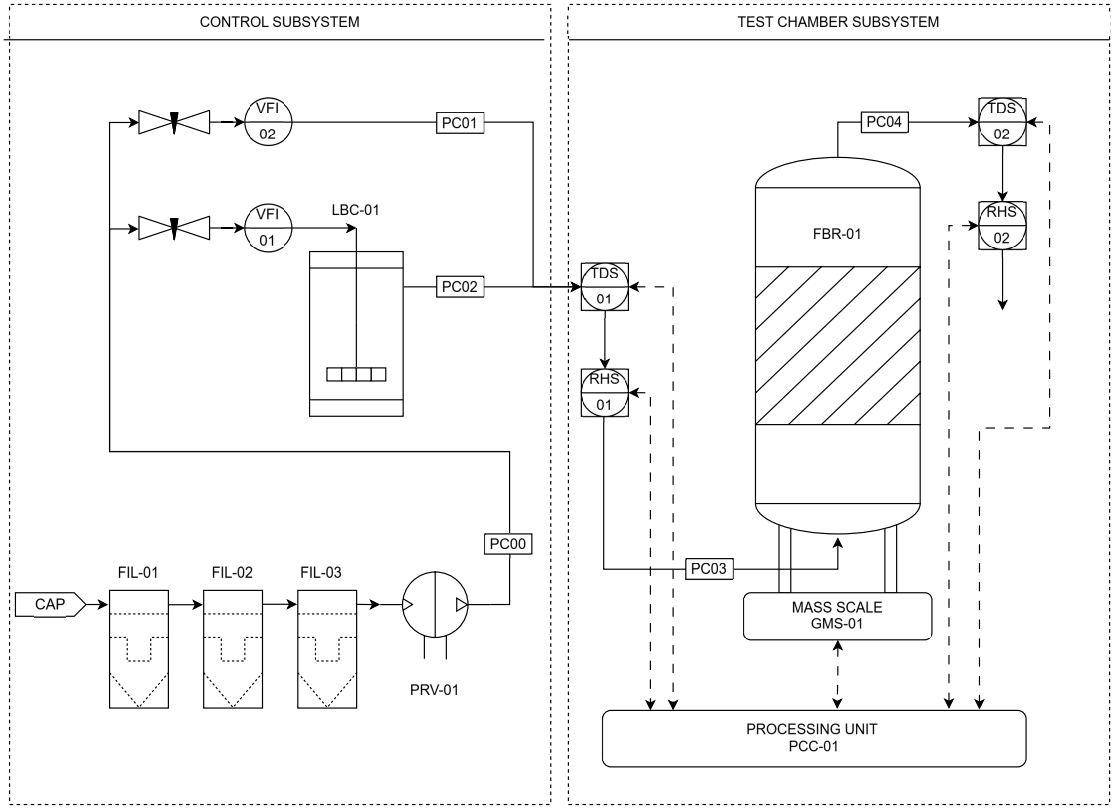

Fig. 2: Process and Instrumentation Diagram of the lab-scale thermochemical heat storage unit. Highlighting main process streams (solid lines), data communication paths (dotted lines), control, and processing units. The diagram presents the units involved in the control of the humid air conditions under the name "Control Subsystem", and the reactor and the monitoring method under the denomination "Test Chamber Subsystem". Detailed information of the components and process line conditions are presented in Tables 1 and 2, respectively.

chemical uptake of water, rather than experimental noise caused by gas flow, temperature variations, pressure changes, or mechanical interference from the tubing, as explained in Section 2.1.

2.4 Hydration of material

Following the preparation phase, the system is ready to be supplied with the working fluid at the required humidity and temperature to initiate the exothermic hydration process. Equilibrium pressure-temperature (P-T) diagrams are used as a reference to determine the precise conditions required to achieve a specific hydration state. For the results presented here, an operational RH of 10% at a constant temperature of 20 °C was selected. The selected conditions lie within the thermodynamic regime favoring hydration of anhydrous $CaCl_2$ toward the tetrahydrate state, based on the equilibrium data reported by Wang et al. (2024). This condition is achieved by adjusting the humidifier's volumetric flow controllers to blend precise ratios of dry and saturated air, as depicted in Figure 2. The hydration process is maintained for at least 12 hours to capture the representative behavior of the fixed bed, considering that total conversion of the material loaded might require prohibitive amounts of time in the experiment due to the different limitations described by Sögütoglu et al. (2021).

After closing the hydration stage, the Nylon holder is removed from the reactor and immediately sealed to prevent further moisture exchange with the environment. The holder and salt are then weighed on a separate laboratory balance to determine the total mass gained. This secondary measurement is later cross-referenced with the continuous dynamic data recorded by the reactor's integrated mass scale.

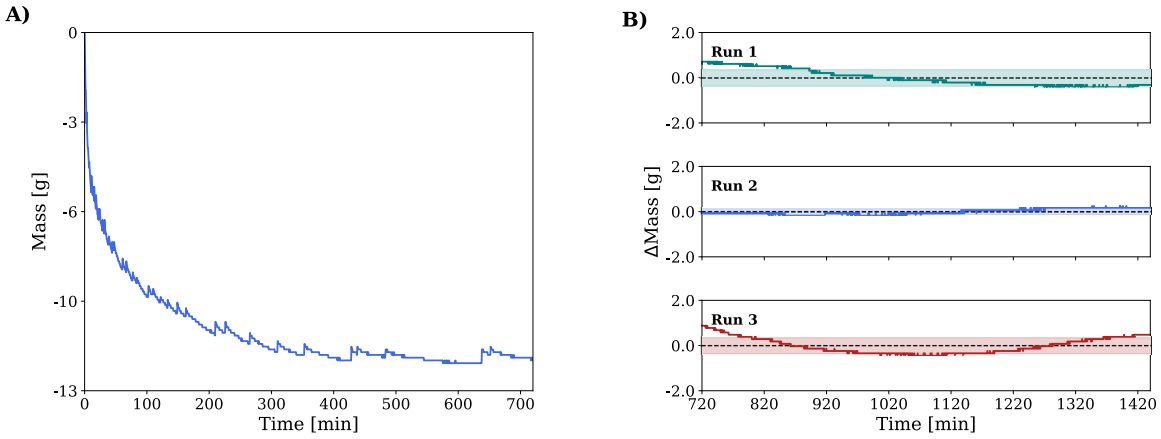

Fig. 3: Macro-gravimetric dynamics over time. A) Mass change profile showing the mass change during the adaptation time, prior to injection of water into the system. B) Mass deviation relative to the average profile across three experimental runs (Run 1, Run 2, Run 3), after adaptation time (720 minutes), once steady state is reached. Solid colored lines indicate recorded mass deviation, dashed black lines represent the mean deviation, and shaded regions denote the $\pm 1\sigma$ standard deviation interval.

3. Results

3.1 Repeatability of inlet conditions

Because the proposed setup integrates multiple analytical methods for TCS applications, validating the reliability of its protocols, control systems, and experimental conditions is essential. To assess the sensor measurements, the experiment was repeated three times under the identical parameters described in Section 2.3. Fresh salt samples from a single, dry-stored batch were used for each run to ensure consistent starting conditions.

Figure 4 presents the inlet temperature and RH of the working fluid at the inlet of the reactor for each of the experimental runs. The repeatable inlet conditions demonstrate the reliability of the control system, with variations remaining largely within one standard deviation of the mean, as shown by the colored band and the dashed line in the figure.

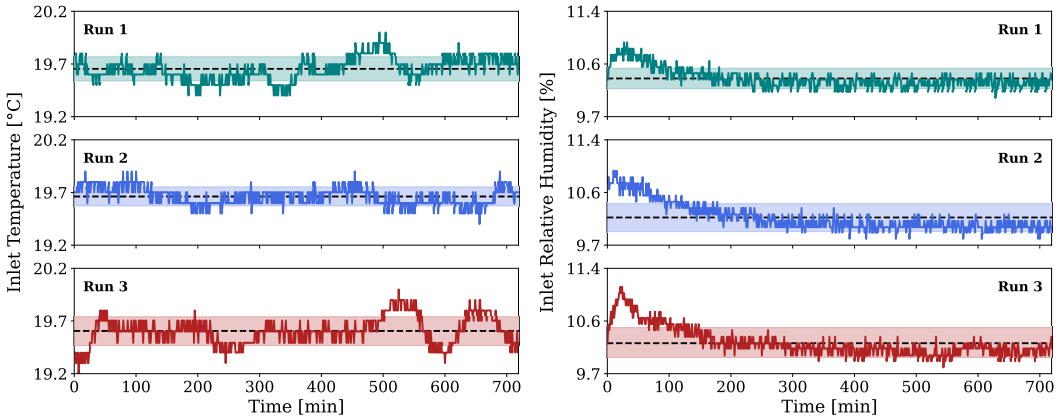

Fig. 4: Measured inlet conditions over time across three experimental runs (Run 1, Run 2, Run 3). Left panels show inlet temperature and right panels show inlet RH. For each run, the solid line indicates the measured data, the dashed black line represents the mean value, and the shaded region denotes the $\pm 1\sigma$ standard deviation.

3.2 Hydration process profiling

Figure 5 illustrates the system's performance during 12 hours of hydration process using the established protocol, where Figure 5A displays the inlet and outlet RH data of the working fluid. Initially, there is a significant difference between the RH values of the process fluid at the inlet and outlet of the reactor, reflecting rapid and efficient water absorption by the TCM bed. Early in the process, the outlet humidity is low. As the

reaction progresses, the solid material absorbs water less efficiently, causing a gradual rise in moisture escaping via the outlet gas stream.

Similarly, Figure 5B shows the temperature of the working fluid at the inlet and outlet of the reactor. The initial sharp rise in outlet temperature corresponds to the exothermic heat of reaction warming the solid bed, which is then carried out of the system by the airflow. This warming phase peaks during the first few minutes, aligning with the maximum rate of water uptake (the largest difference in RH). As hydration in the bed slows, heat generation decreases, causing the outlet temperature to gradually return to the inlet baseline.

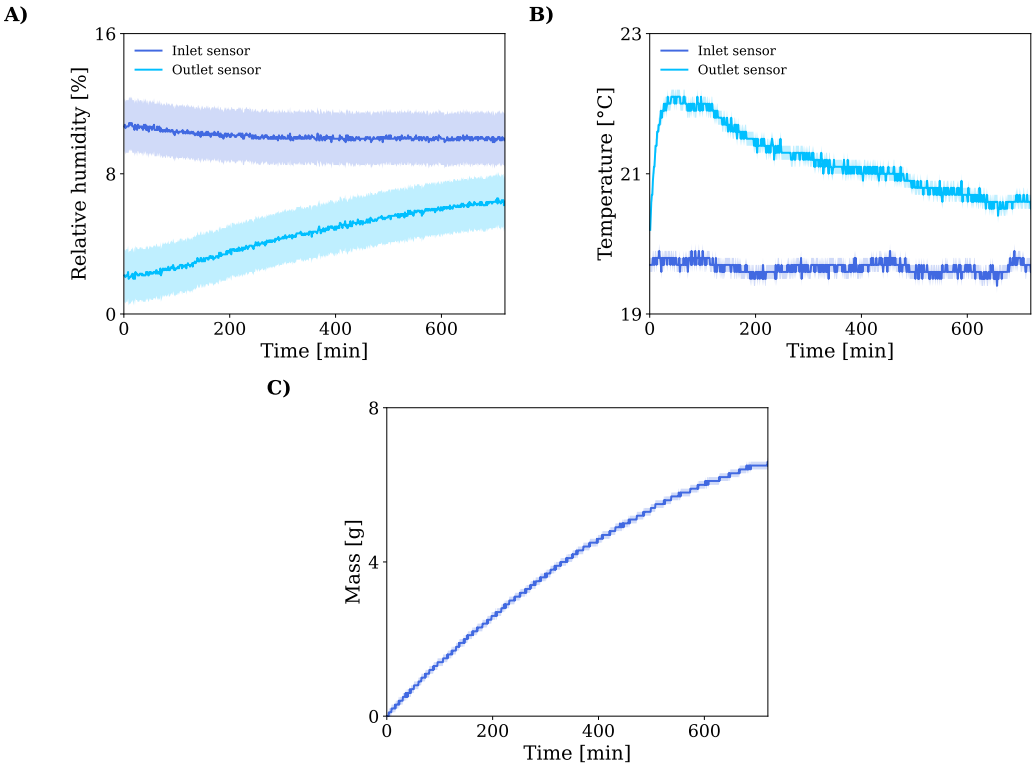

Fig. 5: Experimental monitoring during the salt hydration process. A) Inlet and outlet air stream RH as a function of time. B) Inlet and outlet air stream temperature, displaying an initial exotherm as reaction heat is released. C) Macro-gravimetric measurement showing cumulative mass increase from the uptake of water by the salt fixed-bed over time. Solid lines display the data recorded by the corresponding sensors and the shaded bands present the accuracy intervals given by each device.

Figure 5C presents the continuous macro-gravimetric data, directly showing the progressive mass increase of the moisture taken by the salt. This mass curve inversely mirrors the humidity and temperature trends shown in Figures 5A and 5B. This continuous macro-gravimetric monitoring directly addresses the current challenge of tracking dynamic hydration kinetics in real time, capturing instantaneous water uptake simultaneously with the transient temperature and humidity shifts.

As outlined in Section 2.4, the final salt mass was independently verified using a secondary analytical balance to confirm the accuracy of the in-situ gravimetric data. For the experiment shown in Figure 5, the initial mass of the anhydrous $CaCl_2$ was 100.11 g. After the reaction, the mass of the hydrated salt was 107.56 g, representing a total water gain of 7.45 g. This closely matches the 7.51 g mass increase plotted in Figure 5C, given by the reactor's integrated scale at the end of the experiment.

4. Conclusions

The results presented demonstrate the capability of the proposed macro-gravimetric setup to continuously track water uptake across established hydration boundaries. The direct measurement method reduces reliance on indirect estimation of water uptake from gas-phase measurements and reaction stoichiometry, while providing a continuous reactor-scale measure of bulk hydration.

Repeated experiments under identical operating conditions produced highly consistent profiles, establishing stable baselines and demonstrating strong repeatability for gravimetric, temperature, and RH measurements. The low data dispersion indicates that the integrated sensors detailed in Section 2.1 meet the precision requirements for monitoring lab-scale salt hydration. This accuracy was further confirmed by comparing the in-situ gravimetric data with offline balance measurements in Section 3.2, which showed a deviation of less than 1% for a 100.11 g sample of $CaCl_2$.

The complementary temperature and RH sensors effectively captured the rapid initial exothermic phase and the progressive saturation of the salt bed. These observations align well with findings from similar experimental setups shown in Stengler et al. (2021); Kur et al. (2023); Uykun et al. (2026), validating the reliability of this monitoring protocol. Furthermore, the continuous data streams presented in Figures 5A and B can be used to calculate the extent of the reaction, as proposed by Amrhein et al. (2010). These datasets also support the modeling of kinetic parameters based on mass and heat balances, even in complex scenarios involving additional mass transfer phenomena (Hoang et al. (2020)).

4.1 Research outlook

Preliminary findings confirm that the behavior of bulk salt beds deviates significantly from micro-scale observations when compared to data published in the literature for a similar system (Eberbach et al. (2025); Wang et al. (2024); Molenda et al. (2013)), highlighting the need for robust experimental validation during both hydration and dehydration cycles. Employing the analytical capabilities of the current setup, the next critical step is a comprehensive screening of the reaction phases required to fully hydrate anhydrous $CaCl_2$ to its hexahydrate state, to reach higher temperatures. These experiments will provide key insights into how much the real-world performance of an upscaled device differs from theoretical expectations. Ultimately, this analysis will establish a benchmark for future design optimizations aimed at improving overall system efficiency.

Secondly, to investigate localized phenomena occurring within different sections of the reaction bed, the system will be equipped with a specialized sampling module. This instrument will allow the reacted material to be isolated and securely transported while preserving its precise thermodynamic state at the end of a reaction step. The objective is to transfer the samples to a Micro-CT scanner for high-resolution X-ray tomography. This internal imaging will enable direct visualization of the structural changes and spatial distributions inferred by the macroscopic methods presented in this paper.

References

Michael Amrhein, Nirav Bhatt, Balasubrahmanyan Srinivasan, and Dominique Bonvin. Extents of reaction and flow for homogeneous reaction systems with inlet and outlet streams. *AIChE journal*, 56(11):2873–2886, 2010.

ComWinTop. SHT35 CWT-I2CTH02-35 temperature humidity sensor probe. Product page, a. URL https://store.comwintop.com/products/sht20-sht30-shtc3-sht35-i2c-temperature-humidity-sensor-probe?variant=44316699263203.

ComWinTop. SHT35 CWT-I2CTH03-35-M temperature humidity sensor probe. Product page, b. URL https://store.comwintop.com/products/sht20-sht30-shtc3-sht35-i2c-temperature-humidity-sensor-probe?variant=44316699361507.

DWK Life Sciences. DURAN® gas washing bottle, drechsel type, with filter disc. Product page, Catalogue No. 257040101. URL https://www.dwk.com/duran-gas-washing-bottle-drechsel-type-with-filter-disc.

Michaela C Eberbach, AI Shkatulov, HP Huinink, HR Fischer, and OCG Adan. Hydration pathways of cacl2 inside matrices with different pore sizes. *Microporous and Mesoporous Materials*, 391:113605, 2025.

EMC Pneumatics. EAR series air preparation unit: EAR2000, EAR3000, EAR4000 regulator. Product datasheet, pp. 5.11–5.12. URL https://www.emc-machinery.com/Public/Uploads/uploadfile/files/20251106/EAR4000EAR2000EAR3000Regulator.pdf.

N Ha Hoang, Diogo Rodrigues, and Dominique Bonvin. Revisiting the concept of extents for chemical reaction systems using an enthalpy balance. *Computers & Chemical Engineering*, 136:106652, 2020.

KSI Filtertechnik. KSI ECOCLEAN: Technical data sheet – compressed air filter APF23. Technical Data Sheet Rev. 02_0820, KSI Benelux, August 2020. URL https://ksi-benelux.nl/wp-content/uploads/2021/04/KSI_TDB_APF23_EN_02_0820.pdf. Accessed via KSI Benelux website.

KSI Filtertechnik GmbH. ECOTROC® membrane dryer MT: Solution-oriented compressed air drying. Product Information Rev. 01_0225, KSI Filtertechnik GmbH, Siemensring 54–56, D-47877 Willich, Germany, February 2025. URL https://ksi.eu/wp-content/uploads/2025/10/KSI_PI_MT_EN_01_0225.pdf.

Anti Kur, Jo Darkwa, John Calautit, Rabah Boukhanouf, and Mark Worall. Solid–gas thermochemical energy storage materials and reactors for low to high-temperature applications: a concise review. *Energies*, 16(2): 756, 2023.

Margarethe Molenda, Jana Stengler, Marc Linder, and Antje Wörner. Reversible hydration behavior of cacl2 at high h2o partial pressures for thermochemical energy storage. *Thermochimica acta*, 560:76–81, 2013.

OHAUS Corporation. NAVIGATOR™ portable balances: Multi-purpose portable balances suitable for everyday weighing. Datasheet 8776641_A, OHAUS Corporation, 2020. URL https://dmx.ohaus.com/WorkArea/showcontent.aspx?id=4294992916.

O Opel, HU Rammelberg, M Gérard, and W Ruck. Thermochemical storage materials research-tga/dsc-hydration studies. In *Proceedings of the international conference for sustainable energy storage*, volume 24. Ulster Belfast, 2011.

RS PRO. RS PRO series air flow sensor for air, 0.5L/min min, 5L/min max. RS Components product page, Stock No. 257-6411, a. URL https://nl.rs-online.com/web/p/flow-sensors/2576411.

RS PRO. RS PRO series air flow sensor for air, 4L/min min, 50L/min max. RS Components product page, Stock No. 257-6418, b. URL https://nl.rs-online.com/web/p/flow-sensors/2576418.

Hans Schermeyer, Claudio Vergara, and Wolf Fichtner. Renewable energy curtailment: A case study on today's and tomorrow's congestion management. *Energy Policy*, 112:427–436, 2018.

SCHOTT AG. DURAN®: Tubing, rods and capillaries made of borosilicate glass 3.3. Product Brochure 4Agb01.07.2022KW, SCHOTT AG, Erich-Schott-Strasse 14, 95666 Mitterteich, Germany, July 2022. URL schott.com/duran.

Leyla-Cann Sögütoglu, Felix Birkelbach, Andreas Werner, Hartmut Fischer, Henk Huinink, and Olaf Adan. Hydration of salts as a two-step process: Water adsorption and hydrate formation. *Thermochimica Acta*, 695:178819, 2021.

Jana Stengler, Inga Bürger, and Marc Linder. Performance analysis of a gas-solid thermochemical energy storage using numerical and experimental methods. *International Journal of Heat and Mass Transfer*, 167: 120797, 2021.

Muhammad Priyono Tri Sulistyanto, Kurriawan Budi Pranata, Melania Suweni Muntini Endarko, and Melania Suweni Muntini. Design of electronic mass balance of gram scale using a gage strain sensor. *IJITEE (International Journal of Information Technology and Electrical Engineering)*, 1(3):81–85, 2017.

Awash Tekle Tafere. Thermal energy storage technologies: A review of current landscape and future directions. *F1000Research*, 15:83, 2026.

Zeynep Uykun, Bram Kieskamp, Amir Houshang Mahmoudi, Abhishek Purandare, and Mina Shahi. Suppressing agglomeration in salt hydrate reactors via lattice architecture. *Available at SSRN 6278070*, 2026.

Shaoheng Wang, Amelie Stahlbuhk, and Michael Steiger. Hydration and deliquescence behavior of calcium chloride hydrates. *Fluid Phase Equilibria*, 585:114171, 2024.

Tab. 1: Component Specifications and Operational Parameters

Notation	Function	Catalog name	Model number	Operational range	Reference
FIL-01	Air particle filter	KSI ECOCLEAN Particle Filter	APF26SMA	1–7×10^5 Pa (1-7 bar)	KSI Filtertechnik (2020)
FIL-02	Air oil filter	KSI ECOCLEAN Oil Filter	APF26CA	1–7 ×10^5 Pa (1-7 bar)	KSI Filtertechnik (2020)
FIL-03	Air dryer	KSI ECOTROC Membrane Dryer	MT50	1–12.5 ×10^5 Pa (1-12.5 bar)	KSI Filtertechnik GmbH (2025)
PRV-01	Pressure regulator valve	EMC EAR Series Air Preparation Unit	EAR2000-02	0.5-9 ×10^5 Pa (0.5-9 bar)	EMC Pneumatics
VFI-01	Volumetric flow indicator 01	RS PRO Series Air Flow Sensor	257-6418	0.07-0.84 l/s (4–50 l/min)	RS PRO (b)
VFI-02	Volumetric flow indicator 02	RS PRO Series Air Flow Sensor	257-6411	0.008-0.08 l/s (0.5–5 l/min)	RS PRO (a)
LBC-01	Liquid bubble column	DURAN Gas Washing Bottle (500 cm^3)	257040101	0-1.5 x 10^5 Pa (0-1.5 bar)	DWK Life Sciences
TDS-01	Temperature sensor 01	ComWinTop SHT35	CWT-I2CTH03-35	-40–85 °C	ComWinTop (b)
RHS-01	Relative humidity sensor 01	ComWinTop SHT35	CWT-I2CTH03-35	0–100 %RH	ComWinTop (b)
GMS-01	Mass scale	Ohaus Navigator	NVT6201	0.1–6200 g	OHAUS Corporation (2020)
FBR-01	Fixed bed reactor	Borosilicate Glass Custom-built (500 cm^3)	-	0-2.5 ×10^5 Pa (0-2.5 bar)	SCHOTT AG (2022)
TDS-02	Temperature sensor 02	ComWinTop SHT35	CWT-I2CTH02-35	-40–85 °C	ComWinTop (a)
RHS-02	Relative humidity sensor 02	ComWinTop SHT35	CWT-I2CTH02-35	0–100 %RH	ComWinTop (a)
PCC-01	Processing unit computer	Windows 11			

Tab. 2: Stream conditions notation for Process and Instrumentation Diagram presented in Figure 2.

Notation	Pressure [Pa] ([bar])	VFR l/s ([l/min])	Temperature [°C]	RH [%]
PC00	2×10^5 (2)	-	~20	2.5
PC01	2×10^5 (2)	0.225 (13.5)	~20	2.5
PC02	2×10^5 (2)	0.025 (1.5)	~20	99
PC03	2×10^5 (2)	0.25 (15)	~20	15
PC04	Reacted conditions			